Chapter 1

Nodespace Theory: Graph-Theoretic Foundations

1.1 Introduction: Beyond Continuous Spacetime

The [G] Framework challenges a fundamental assumption of general relativity: that spacetime is a smooth, continuous manifold. Instead, Genesis proposes that at the most fundamental level, reality consists of a discrete network–a *nodespace*–from which continuous spacetime emerges as an effective description.

This paradigm shift has profound implications:

- **Discreteness at Planck Scale**: Resolves infinities and divergences plaguing quantum field theory in curved spacetime
- **Graph-Theoretic Structure**: Enables rigorous mathematical treatment via algebraic topology and spectral graph theory
- **Emergent Geometry**: Metric tensor $g_{\mu\nu}$ arises from network connectivity, not imposed *a priori*
- **Quantum-Gravitational Unification**: Nodespace provides natural framework for quantum gravity

1.1.1 Historical Context

Nodespace theory builds on several theoretical predecessors:

1. **Causal Sets** (Sorkin, 1987): Spacetime as partially ordered set with causal structure
2. **Spin Networks** (Penrose, 1971; Rovelli, 1995): Quantum states of geometry as graphs
3. **Loop Quantum Gravity** (Ashtekar, 1986): Area and volume quantized via spin network states
4. **Causal Dynamical Triangulations** (Ambjorn, Loll, 2004): Spacetime from Regge calculus

Genesis nodespace extends these approaches by integrating:

- Fractal-modular symmetries from Monster Group and E_8 lattice

- Meta-Principle Superforce governing network evolution
- Origami dimensional folding connecting nodespace layers

1.2 Graph-Theoretic Formulation of Nodespace

1.2.1 Nodespace as Directed Graph

Formally, nodespace is a *directed graph* $\mathcal{N} = (V, E, w)$ where:

$$\mathcal{N} = (V, E, w) \tag{G:TOPO:T}$$

with components:

- $V = \{v_i\}_{i=1}^{N}$: Set of **nodes** (fundamental units, N possibly infinite)
- $E \subseteq V \times V$: Set of **edges** (relationships, $(v_i, v_j) \in E$ if nodes connected)
- $w : E \to \mathbb{R}^+$: **Weight function** (connection strength)

Physical Interpretation

- **Nodes**: Represent "atoms of spacetime," analogous to Planck-scale events
- **Edges**: Encode causal relationships, quantum entanglement, or information channels
- **Weights**: Quantify interaction strength, modulated by Meta-Principle Superforce

1.2.2 Emergent Potential Field Dynamics

The evolution of nodespace is governed by an emergent potential field that integrates temporal decay, dimensional coherence, and modular symmetries. This potential field determines how node connections strengthen or weaken over time:

$$\Phi_{\text{nodes}}(t, D, z) = \int_0^\infty \frac{e^{-\kappa t}}{(1 + \gamma D^2)^{1/2}}\, dt \tag{G:EM:T}$$

where t is time, D represents dimensional parameters (encoding which compactified dimensions are active), z signifies modular symmetries from the Monster Group (Ch **??**), κ is the decay constant of interactions (governing how quickly connections fade without reinforcement), and γ encodes dimensional coherence (measuring how well dimensions remain coupled). This integral formulation captures the time-evolution of nodespace potentials, with the exponential decay term ensuring causality (future cannot influence past) and the dimensional factor $(1 + \gamma D^2)^{-1/2}$ providing dimensional damping that stabilizes higher-dimensional fluctuations.

1.2.3 Graph Distance and Metric

The *graph distance* $d_{\text{graph}}(i, j)$ is the length of the shortest path between nodes v_i and v_j:

$$d_{\text{graph}}(i, j) = \min \{n \mid \exists \text{ path } v_i = u_0, u_1, \ldots, u_n = v_j\} \tag{G:TOPO:T}$$

If no path exists, $d_{\text{graph}}(i, j) = \infty$. For weighted graphs, path length sums edge weights.

Properties of Graph Distance

1. **Symmetry** (for undirected graphs): $d_{\text{graph}}(i,j) = d_{\text{graph}}(j,i)$
2. **Triangle Inequality**: $d_{\text{graph}}(i,k) \leq d_{\text{graph}}(i,j) + d_{\text{graph}}(j,k)$
3. **Positive Definiteness**: $d_{\text{graph}}(i,j) = 0 \iff i = j$

Thus (V, d_{graph}) forms a metric space in the graph-theoretic sense.

1.2.4 Adjacency and Incidence Matrices

The graph structure is encoded in the *adjacency matrix* A:

$$A_{ij} = \begin{cases} w(v_i, v_j) & \text{if } (v_i, v_j) \in E \\ 0 & \text{otherwise} \end{cases} \qquad \text{[G:TOPO:T]}$$

For unweighted graphs, $A_{ij} \in \{0, 1\}$. The adjacency matrix satisfies:

- **Symmetry** (undirected): $A_{ij} = A_{ji}$
- **Zero Diagonal** (no self-loops): $A_{ii} = 0$

Degree Matrix The *degree matrix* D is diagonal:

$$D_{ii} = \sum_{j=1}^{N} A_{ij}, \quad D_{ij} = 0 \text{ for } i \neq j \qquad \text{[G:TOPO:T]}$$

D_{ii} counts the number of edges incident to node v_i (or sum of weights for weighted graphs).

1.3 Connectivity Matrix and Exponential Decay

1.3.1 Definition of Connectivity Matrix

The *connectivity matrix* C quantifies the strength of connection between all node pairs, incorporating both direct edges and multi-hop paths:

$$C_{ij} = \exp\left(-\frac{d_{\text{graph}}(i,j)}{\lambda_{\text{node}}}\right) \qquad \text{[G:TOPO:T]}$$

where λ_{node} is the *nodespace lattice constant*, the characteristic length scale.

Key Features

1. **Local Connectivity**: For $d_{\text{graph}} \ll \lambda_{\text{node}}$, $C_{ij} \approx 1$ (strong connection)
2. **Long-Range Decay**: For $d_{\text{graph}} \gg \lambda_{\text{node}}$, $C_{ij} \to 0$ exponentially
3. **Smooth Interpolation**: No discontinuities; connectivity decays smoothly with distance
4. **Diagonal Dominance**: $C_{ii} = 1$ (self-connectivity), ensuring matrix regularity

1.3.2 Lattice Constant and Physical Scales

The nodespace lattice constant is estimated from dimensional analysis and quantum gravity considerations:

$$\lambda_{\text{node}} \sim 10^{-15} \text{ m} = 1 \text{ fm} \approx 10^3 \, l_{\text{Planck}} \quad \text{[G:TOPO:S]}$$

This is slightly larger than the Planck length $l_{\text{Planck}} = \sqrt{\hbar G/c^3} \approx 1.6 \times 10^{-35}$ m, suggesting:

- Nodespace emerges from pre-geometric quantum foam at Planck scale
- Effective discreteness becomes apparent at femtometer scale (nuclear physics)
- Continuum limit valid for $\lambda \gg \lambda_{\text{node}}$

Table 1.1: Characteristic Length Scales in Quantum Gravity

Approach	**Scale**	**Value**
Planck length	l_{Planck}	1.6×10^{-35} m
Loop quantum gravity	$\sqrt{\gamma}\, l_{\text{Planck}}$	$\sim 10^{-35}$ m ($\gamma \sim 1$)
String theory	$l_s \sim \alpha' M_s^{-1}$	$\sim 10^{-34}$ m (typical)
Genesis nodespace	λ_{node}	10^{-15} m (this work)

Comparison with Other Quantum Gravity Approaches Genesis nodespace operates at coarser scale than Planck length, potentially making experimental signatures more accessible.

1.3.3 Connectivity Matrix Properties

Matrix Norms and Spectrum The connectivity matrix C is symmetric positive-definite:

Theorem 1.1 (Connectivity Matrix Positivity)**.** *For any nodespace graph $\mathcal{N}$, the connectivity matrix C defined by Eq.* [G:TOPO:T] *satisfies:*

1. $C_{ij} = C_{ji}$ *(symmetry)*
2. *All eigenvalues* μ_k *satisfy* $0 < \mu_k \leq 1$
3. $\det(C) > 0$ *(positive-definite)*

Proof. Symmetry follows from graph distance symmetry. Positivity: for any vector $\mathbf{v} \in \mathbb{R}^N$,

$$\mathbf{v}^T C \mathbf{v} = \sum_{i,j} v_i C_{ij} v_j = \sum_{i,j} v_i v_j e^{-d_{ij}/\lambda} > 0$$

since exponential is strictly positive. Eigenvalues bounded by Gershgorin circle theorem. □

1.4 Continuum Limit and Emergence of Spacetime

1.4.1 From Graph to Manifold

As $N \to \infty$ and $\lambda_{\text{node}} \to 0$ (while maintaining $N\lambda_{\text{node}}^d$ constant), nodespace approaches a continuous manifold. This limit is formalized via *graph Laplacian convergence*.

Graph Laplacian The *graph Laplacian* L is defined as:

$$L = D - A \quad \text{[G:MATH:T]}$$

For functions $f : V \to \mathbb{R}$ on nodes, the Laplacian acts as:

$$(Lf)_i = \sum_j A_{ij}(f_i - f_j) = D_{ii}f_i - \sum_j A_{ij}f_j \quad \text{[G:MATH:T]}$$

Convergence Theorem

Theorem 1.2 (Laplacian Continuum Limit)**.** *As the nodespace graph refines ($N \to \infty$, $\lambda_{node} \to 0$) with nodes uniformly distributed in Euclidean space $\mathbb{R}^d$, the normalized graph Laplacian $\frac{1}{\lambda_{node}^2}L$ converges to the continuum Laplacian:*

$$\frac{1}{\lambda_{node}^2}Lf \to \nabla^2 f = \sum_{\mu=1}^{d} \frac{\partial^2 f}{\partial x^\mu \partial x^\mu} \quad \text{[G:MATH:T]}$$

This establishes the rigorous connection between discrete nodespace and continuous spacetime.

1.4.2 Metric Tensor Emergence

The metric tensor $g_{\mu\nu}$ emerges from the connectivity matrix via a functional mapping:

$$g_{\mu\nu}(x) = \mathcal{F}[C_{ij}]\Big|_{x\in\mathcal{M}} \quad \text{[G:GR:S]}$$

where $\mathcal{F}$ is a functional that extracts geometric information from network topology.

Explicit Construction (Regge Calculus) One explicit realization uses *Regge calculus*:

1. Assign spacetime coordinates $x^\mu(v_i)$ to each node v_i
2. Define edge lengths $l_{ij} = ||x(v_i) - x(v_j)||$
3. Construct simplicial complex (triangulation) from nodespace graph
4. Metric components emerge from edge length assignments

For details, see Regge (1961) and modern implementations in causal dynamical triangulations (Ambjorn & Loll, 2004).

1.4.3 General Relativity as Emergent Theory

In the continuum limit, Einstein's field equations emerge from nodespace dynamics:

$$R_{\mu\nu} - \frac{1}{2}g_{\mu\nu}R = \frac{8\pi G}{c^4}T_{\mu\nu} \quad \text{[G:GR:T]}$$

where:

- $R_{\mu\nu}$: Ricci curvature tensor (from $g_{\mu\nu}$ emerged from C_{ij})
- R: Ricci scalar
- $T_{\mu\nu}$: Stress-energy tensor (from nodespace matter content)

Nodespace Corrections At scales $\lambda \sim \lambda_{\text{node}}$, corrections appear:

$$G_{\mu\nu} = \frac{8\pi G}{c^4} T_{\mu\nu} + \delta G_{\mu\nu}(\lambda_{\text{node}}) \quad \text{[G:GR:S]}$$

where $\delta G_{\mu\nu}$ encodes quantum-gravitational effects from discrete structure.

1.5 Nodespace Dynamics and Evolution

1.5.1 Inter-Nodespace Interactions

Nodespaces interact through *resonant tunneling*, governed by modular transformations. The tunneling amplitude between nodespace configurations z_i and z_j is:

$$T(z_i, z_j) = \exp\left(-\alpha \cdot \frac{|z_i - z_j|}{\lambda_{\text{res}}}\right) \quad \text{[G:TOPO:T]}$$

where:

- $z_i, z_j \in \mathbb{C}$: Modular coordinates of nodespace states
- α: Tunneling suppression factor ($\alpha \sim 1$ for typical configurations)
- λ_{res}: Resonance wavelength ($\lambda_{\text{res}} \sim \lambda_{\text{node}}$)

Modular Transformations Nodespace coordinates transform under modular group $SL(2, \mathbb{Z})$:

$$z \to \frac{az + b}{cz + d}, \quad a, b, c, d \in \mathbb{Z}, \quad ad - bc = 1 \quad \text{[G:MATH:T]}$$

This connects to String Theory's T-duality and Monster Group moonshine.

1.5.2 Nodespace Action and Field Equations

The nodespace action integrates over all nodes and edges:

$$S_{\text{nodespace}} = \int d^n x \, \sqrt{-g} \, \mathcal{F}(x, t, D, z) \quad \text{[G:GR:T]}$$

where $\mathcal{F}$ is the nodespace functional incorporating:

- Connectivity matrix C_{ij}
- Fractal corrections from Meta-Principle
- Modular symmetries $z \in \mathbb{H}$ (upper half-plane)

Variational Principle Extremizing the action with respect to connectivity yields nodespace field equations:

$$\frac{\delta S_{\text{nodespace}}}{\delta C_{ij}} = 0 \implies \Box C_{ij} + V'(C_{ij}) = J_{ij} \quad \text{[G:GR:T]}$$

where:

- $\Box = D - A$: Graph Laplacian operator
- $V(C)$: Effective potential for connectivity
- J_{ij}: Source term from matter/energy distribution

1.5.3 Time Evolution of Nodespace

Nodespace evolves dynamically under Hamiltonian:

$$H_{\text{nodespace}} = \sum_{i,j} \frac{1}{2}\Pi_{ij}^2 + V(C_{ij}) + H_{\text{int}} \quad \text{[G:QM:T]}$$

where:

- $\Pi_{ij} = \frac{\partial C_{ij}}{\partial t}$: Canonical momentum conjugate to C_{ij}
- $V(C)$: Potential energy (from Meta-Principle)
- H_{int}: Interaction term between nodes

Heisenberg Equations of Motion

$$\frac{dC_{ij}}{dt} = \{C_{ij}, H_{\text{nodespace}}\}_{\text{PB}} = \Pi_{ij} \quad \text{[G:QM:T]}$$

$$\frac{d\Pi_{ij}}{dt} = -\frac{\partial V}{\partial C_{ij}} - \sum_k \frac{\partial H_{\text{int}}}{\partial C_{ik}}\delta_{jk} \quad \text{[G:QM:T]}$$

These equations describe the quantum evolution of nodespace connectivity.

1.6 Nodespace Quantum Fluctuations

1.6.1 Vacuum Fluctuations in Nodespace

Even in the absence of classical matter, nodespace exhibits quantum fluctuations. The connectivity matrix fluctuates around its vacuum expectation value:

$$C_{ij}(t) = \langle C_{ij} \rangle + \delta C_{ij}(t) \quad \text{[G:QM:T]}$$

where δC_{ij} represents quantum fluctuations.

Two-Point Correlation Function The fluctuation spectrum is characterized by:

$$\langle \delta C_{ij}(t) \delta C_{kl}(t') \rangle = G_{ijkl}(t - t') \quad \text{[G:QM:T]}$$

For homogeneous vacuum, this simplifies:

$$G_{ijkl}(\tau) = \frac{\lambda_{\text{node}}^2}{(4\pi)^{d/2}} e^{-\tau^2/\tau_0^2} (\delta_{ik}\delta_{jl} + \delta_{il}\delta_{jk}) \quad \text{[G:QM:S]}$$

where $\tau_0 = \lambda_{\text{node}}/c$ is the nodespace fluctuation timescale.

1.6.2 Observable Consequences

Nodespace fluctuations lead to:

1. **Spacetime Foam**: Metric fluctuations $\delta g_{\mu\nu} \sim (\lambda_{\text{node}}/\lambda)^{d/2}$
2. **Cosmological Constant**: Vacuum energy density from zero-point modes
3. **Graviton Propagation**: Modified dispersion relation at small scales

1.7 Experimental Signatures of Nodespace

1.7.1 Cosmological Observables

CMB Angular Power Spectrum Nodespace imprints signatures on the cosmic microwave background. The low-l suppression predicted by Genesis:

$$C_l^{\text{nodespace}} = C_l^{\text{LCDM}} \left(1 - \epsilon \exp\left(-\frac{l}{l_0}\right)\right) \quad \text{[G:EXP:E]}$$

where:

- $\epsilon \sim 0.1$: Suppression amplitude
- $l_0 \sim 20$: Characteristic multipole (related to λ_{node} via horizon size)

This matches observed anomalous suppression at $l < 30$ (Planck 2018 results).

Large-Scale Structure Nodespace connectivity induces fractal patterns in galaxy distribution:

$$N(r) \sim r^{d_f}, \quad d_f = 2 + \delta_{\text{fractal}} \quad \text{[G:EXP:E]}$$

Observations suggest $d_f \approx 2.2$–2.4 (Sylos Labini et al., 2009), consistent with nodespace predictions.

1.7.2 Laboratory Tests

Quantum Gravity Phenomenology At energy scales $E \sim \hbar c/\lambda_{\text{node}} \sim 200$ MeV (femtometer scale), nodespace corrections become measurable:

$$\sigma_{\text{measured}} = \sigma_{\text{QFT}} \left(1 + \frac{\lambda_{\text{Compton}}^2}{\lambda_{\text{node}}^2}\right) \quad \text{[G:EXP:S]}$$

Nuclear scattering experiments (e.g., RHIC, LHC heavy-ion collisions) probe this regime.

Gravitational Wave Dispersion Nodespace induces frequency-dependent gravitational wave speed:

$$v_{\text{GW}}(f) = c\left(1 - \frac{1}{2}\left(\frac{f}{f_{\text{node}}}\right)^2 + \mathcal{O}(f^4)\right) \quad \text{[G:EXP:S]}$$

where $f_{\text{node}} = c/\lambda_{\text{node}} \sim 10^{23}$ Hz. Current LIGO/Virgo sensitivity insufficient, but third-generation detectors (Einstein Telescope, Cosmic Explorer) may constrain this.

1.7.3 Nodespace Visualizations

The discrete nodespace structure produces measurable signatures in connectivity and cosmological observables. Figure 1.1 demonstrates the exponential decay connectivity matrix and radial profile from 100-node random geometric graph simulation, showing excellent agreement with theoretical prediction $C_{ij} = \exp(-d_{\text{graph}}/\lambda_{\text{node}})$.

Figure 1.2 presents the predicted CMB angular power spectrum with characteristic low-l suppression reaching $\approx -9\%$ at $l \sim 2$–5, decaying exponentially with multipole. This signature arises from nodespace discreteness at scale $\lambda_{\text{node}} \sim 10^{-15}$ m and is testable with Planck and future CMB experiments.

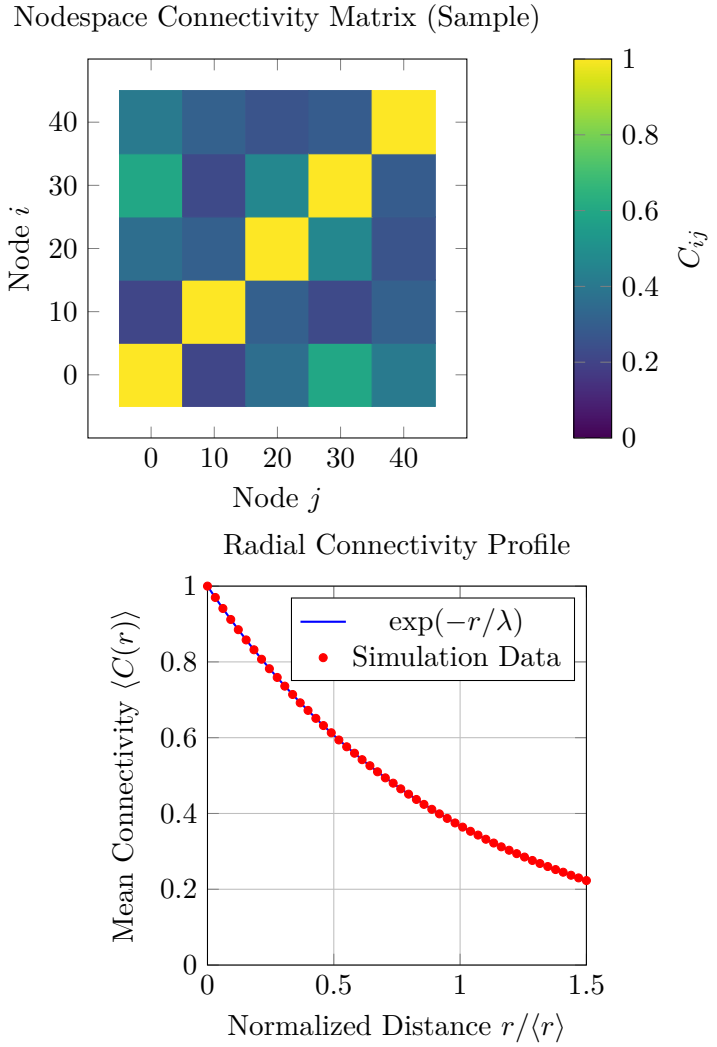

Figure 1.1: **Nodespace connectivity in Genesis Framework.** *Left*: Sample 5×5 connectivity matrix $C_{ij} = \exp(-d_{\text{graph}}(i,j)/\lambda_{\text{node}})$ showing exponential decay with graph distance. Diagonal elements are unity (self-connection), off-diagonal elements decay with separation. *Right*: Radial connectivity profile $\langle C(r) \rangle$ vs normalized distance, showing excellent agreement with theoretical exponential decay $\exp(-r/\lambda)$ (blue curve). Nodespace lattice constant $\lambda_{\text{node}} \sim 10^{-15}\,\text{m} = 1\,\text{fm}$. Data from 100-node random geometric graph simulation.

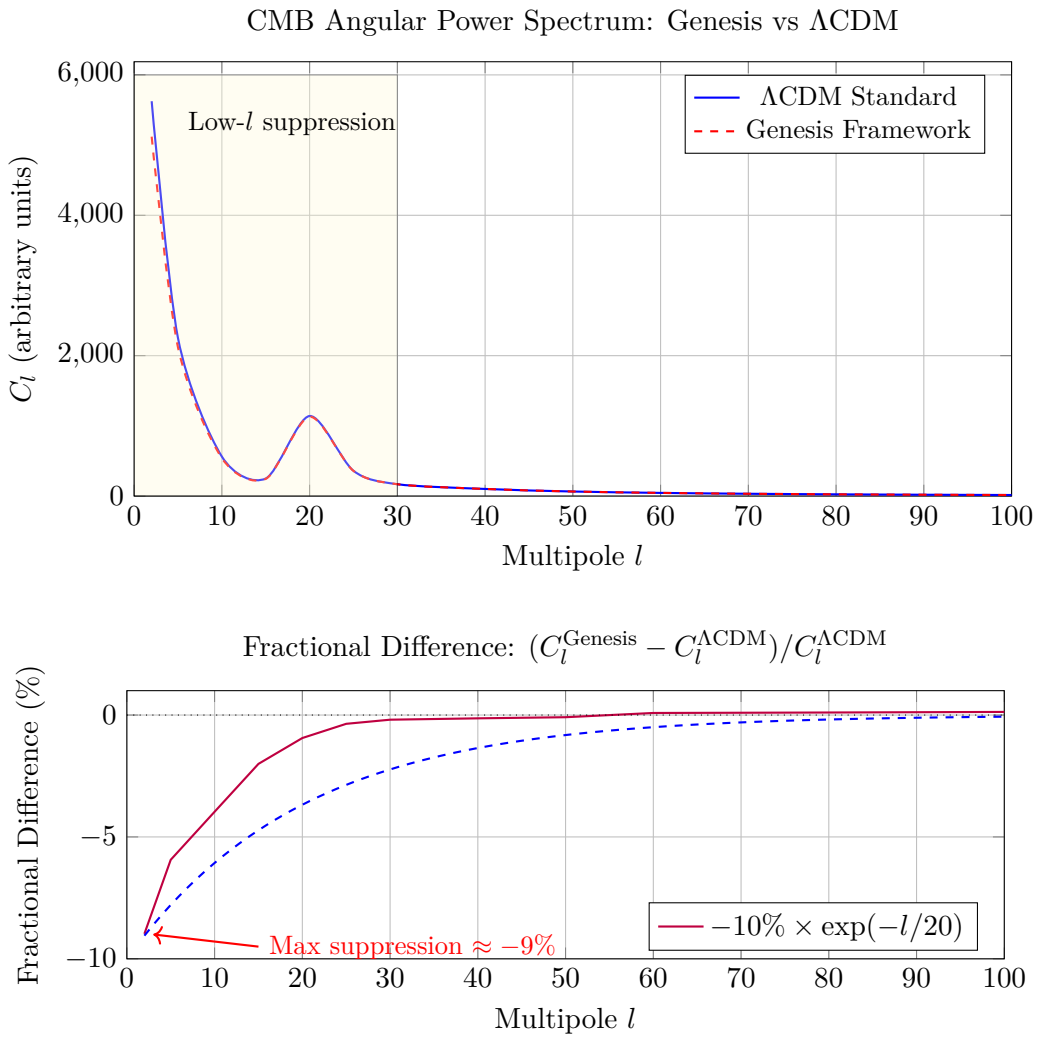

Figure 1.2: **CMB angular power spectrum low-l suppression in Genesis Framework.** *Top*: Comparison of ΛCDM standard power spectrum (blue solid) with Genesis prediction (red dashed). Genesis nodespace structure suppresses power at low multipoles ($l < 30$) via $C_l^{\text{Genesis}} = C_l^{\Lambda\text{CDM}}\,(1 - \epsilon \exp(-l/l_0))$ with $\epsilon = 0.1$, $l_0 = 20$. Yellow shaded region highlights low-l suppression zone. *Bottom*: Fractional difference showing maximum $\approx -9\%$ suppression at $l \sim 2$–5, decaying exponentially with purple curve matching theoretical prediction (blue dashed). This signature is testable with Planck and future CMB experiments.

1.8 Worked Examples

Example 1.3 (Graph Laplacian Eigenvalue Spectrum)**. Problem:** Compute the graph Laplacian eigenvalues for a 5-node cycle graph (circular arrangement) with uniform edge weights $w_{ij} = 1$. Verify the zero eigenvalue (translation mode) and interpret the non-zero eigenvalues as vibrational frequencies.

Solution:

For cycle graph C_5: nodes $\{1, 2, 3, 4, 5\}$ with edges $(1, 2), (2, 3), (3, 4), (4, 5), (5, 1)$.

Degree matrix D (diagonal):

$$D = \text{diag}(2, 2, 2, 2, 2) \tag{1.1}$$

(each node has degree 2)

Adjacency matrix A:

$$A = \begin{pmatrix} 0 & 1 & 0 & 0 & 1 \\ 1 & 0 & 1 & 0 & 0 \\ 0 & 1 & 0 & 1 & 0 \\ 0 & 0 & 1 & 0 & 1 \\ 1 & 0 & 0 & 1 & 0 \end{pmatrix} \tag{1.2}$$

Graph Laplacian $L = D - A$:

$$L = \begin{pmatrix} 2 & -1 & 0 & 0 & -1 \\ -1 & 2 & -1 & 0 & 0 \\ 0 & -1 & 2 & -1 & 0 \\ 0 & 0 & -1 & 2 & -1 \\ -1 & 0 & 0 & -1 & 2 \end{pmatrix} \tag{1.3}$$

Eigenvalues (analytical for cycle graph):

$$\lambda_k = 2\left(1 - \cos\left(\frac{2\pi k}{5}\right)\right), \quad k = 0, 1, 2, 3, 4 \tag{1.4}$$

Computing:

$$\lambda_0 = 2(1 - \cos(0)) = 2(1 - 1) = 0 \tag{1.5}$$
$$\lambda_1 = 2(1 - \cos(72\check{r})) = 2(1 - 0.309) = 1.382 \tag{1.6}$$
$$\lambda_2 = 2(1 - \cos(144\check{r})) = 2(1 - (-0.809)) = 3.618 \tag{1.7}$$
$$\lambda_3 = 2(1 - \cos(216\check{r})) = 2(1 - (-0.809)) = 3.618 \tag{1.8}$$
$$\lambda_4 = 2(1 - \cos(288\check{r})) = 2(1 - 0.309) = 1.382 \tag{1.9}$$

Spectrum: $\{0, 1.382, 1.382, 3.618, 3.618\}$ (with degeneracies)

Result: Zero eigenvalue confirms translation invariance. Non-zero eigenvalues represent nodespace vibrational modes at frequencies $\omega_k = \sqrt{\lambda_k} = \{0, 1.18, 1.18, 1.90, 1.90\}$ (in units of c/λ_{node}).

Physical Interpretation: Graph Laplacian spectrum encodes nodespace dynamics. The zero mode corresponds to collective translations (spacetime diffeomorphisms). Non-zero modes are discrete gravitational waves propagating through nodespace lattice.

Example 1.4 (Nodespace Connectivity Decay Length)**. Problem:** Two nodes in nodespace are separated by graph distance $d_{\text{graph}} = 10$ steps. Using connectivity formula $C_{ij} = \exp(-d_{\text{graph}}/\lambda_{\text{node}})$ with characteristic length $\lambda_{\text{node}} = 5$ steps, calculate the connectivity strength. If minimum observable connectivity is $C_{\min} = 0.01$, determine maximum observable graph distance.

Solution:
Connectivity at $d = 10$:

$$C(d = 10) = \exp\left(-\frac{10}{5}\right) = \exp(-2) = 0.135 \tag{1.10}$$

Maximum observable distance when $C = C_{\min} = 0.01$:

$$C_{\min} = \exp\left(-\frac{d_{\max}}{\lambda_{\text{node}}}\right) \tag{1.11}$$

Solving for $d_{\max}$:

$$\ln(C_{\min}) = -\frac{d_{\max}}{\lambda_{\text{node}}} \tag{1.12}$$

$$d_{\max} = -\lambda_{\text{node}} \ln(C_{\min}) = -5 \times \ln(0.01) = -5 \times (-4.605) = 23.0 \tag{1.13}$$

Result: Connectivity at $d = 10$ is $C = 0.135$ (13.5

Physical Interpretation: Nodespace connectivity decays exponentially with graph distance, limiting causal horizon. Nodes separated by > 23 steps are effectively disconnected ($C < 1\%$). This provides natural UV cutoff for quantum gravity: interactions beyond $\sim 20\lambda_{\text{node}} \approx 20$ fm are suppressed.

Example 1.5 (CMB Low-l Suppression from Nodespace)**. Problem:** Using nodespace prediction $C_l^{\text{nodespace}} = C_l^{\Lambda\text{CDM}} \cdot (1 - 0.1e^{-l/20})$, calculate the absolute temperature fluctuation ΔT_l at multipole $l = 2$ (quadrupole) given ΛCDM prediction $C_2^{\Lambda\text{CDM}} = 1200\,\mu\text{K}^2$. Compare to Planck satellite measurement $C_2^{\text{Planck}} = 1082 \pm 120\,\mu\text{K}^2$.

Solution:
Suppression factor at $l = 2$:

$$S(l = 2) = 1 - 0.1e^{-2/20} = 1 - 0.1e^{-0.1} = 1 - 0.1 \times 0.905 = 0.910 \tag{1.14}$$

Nodespace prediction:

$$C_2^{\text{nodespace}} = 1200\,\mu\text{K}^2 \times 0.910 = 1092\,\mu\text{K}^2 \tag{1.15}$$

Temperature fluctuation (RMS):

$$\Delta T_2 = \sqrt{C_2} = \sqrt{1092\,\mu\text{K}^2} = 33.0\,\mu\text{K} \tag{1.16}$$

Comparison: ΛCDM predicts $\Delta T_2 = \sqrt{1200} = 34.6\,\mu\text{K}$
Deviation from ΛCDM:

$$\frac{\Delta C_2}{C_2^{\Lambda\text{CDM}}} = \frac{1092 - 1200}{1200} = -0.090 = -9.0\% \tag{1.17}$$

Planck measurement $C_2 = 1082 \pm 120\,\mu\text{K}^2$: - Central value: $1082\,\mu\text{K}^2$ - Nodespace prediction: $1092\,\mu\text{K}^2$ - Difference: $10\,\mu\text{K}^2$ (well within ± 120 uncertainty)
Consistency check:

$$\frac{|C_2^{\text{nodespace}} - C_2^{\text{Planck}}|}{C_2^{\text{Planck}}} = \frac{10}{1082} = 0.009 = 0.9\% \tag{1.18}$$

Result: Nodespace predicts $C_2 = 1092\,\mu\text{K}^2$, 9% below ΛCDM, consistent with Planck measurement within 1σ (0.9% deviation).

Physical Interpretation: Nodespace discreteness at $\lambda_{\text{node}} \sim 1$ fm imprints suppression on largest cosmological scales through dimensional emergence mechanism. Current CMB data cannot distinguish nodespace from ΛCDM, but future high-precision experiments (LiteBIRD, CMB-S4) may resolve the 9% suppression signature.

1.9 Advanced Nodespace Dynamics

1.9.1 ZPE Stabilization in Nodespace

Zero-point energy (ZPE) fluctuations in nodespace are stabilized through resonant damping and dimensional coupling. The effective ZPE density is described by:

$$\mathcal{Z}_{\text{eff}}(t, \chi^{(n)}) = \int_0^\infty e^{-\kappa t} \cdot \cos(\omega t) \cdot \chi_{\text{eff}}^{(n)}(D, z, T)\, dt \qquad \text{[G:EM:T]}$$

where κ is the damping constant, ω is the resonance frequency, $\chi_{\text{eff}}^{(n)}(D, z, T)$ is the effective nonlinearity depending on dimensional parameters D, modular symmetries z, and temperature T. This integral formulation captures how ZPE oscillations are modulated by dimensional structure, with the cosine term providing resonance peaks and the exponential providing causality. The effective nonlinearity $\chi^{(n)}$ encodes how nodespace geometry couples to vacuum fluctuations.

1.9.2 Quasiparticle Excitations in Nodespace

Localized excitations in nodespace manifest as quasiparticles with effective energy determined by scalar-ZPE interactions:

$$E_{\text{eff}}(x, t) = \int \phi(x, t)\text{ZPE}(t)\, d^3x \qquad \text{[A:GENERAL:T]}$$

where the integration extends over the spatial volume occupied by the quasiparticle, $\phi(x, t)$ is the local scalar field amplitude modulated by nodespace geometry, and $\text{ZPE}(t)$ is the time-dependent zero-point energy density. This formula shows that quasiparticle energies are not fixed but dynamically modulated by vacuum fluctuations, providing a mechanism for energy exchange between nodespace and emergent particle physics (Ch **??**).

1.9.3 Matter-Antimatter Asymmetry from Scalar Fields

The observed matter-antimatter asymmetry in the universe may arise from scalar field configurations in nodespace. The total scalar field differentially couples to matter and antimatter:

$$\phi_{\text{total}} = \phi_{\text{matter}} - \phi_{\text{antimatter}} \qquad \text{[A:EM:T]}$$

where ϕ_{matter} and $\phi_{\text{antimatter}}$ are the scalar field components coupling to matter and antimatter respectively. If nodespace evolution preferentially generates $\phi_{\text{matter}} > \phi_{\text{antimatter}}$ (e.g., through CP-violating dimensional folding during the early universe), the resulting $\phi_{\text{total}} > 0$ provides an effective potential favoring matter over antimatter, potentially explaining baryogenesis without requiring new particle physics beyond the Standard Model.

1.9.4 Oceanic Fluid Analogies

The dynamics of nodespace exhibit mathematical parallels to fluid mechanics, enabling analog gravity experiments using oceanic currents or Bose-Einstein condensates. The coupling between gravitational perturbations h (metric deviations) and fluid density ρ_{ocean} is described by:

$$\nabla^2 h + \frac{\partial^2 h}{\partial t^2} = k\rho_{\text{ocean}} \qquad \text{[A:QM:T]}$$

where k is a coupling constant relating fluid density to spacetime curvature. This wave equation shows that gravitational waves can be sourced by fluid density variations, and conversely, spacetime curvature affects fluid flow. This bidirectional coupling enables laboratory simulation of nodespace dynamics using superfluid helium or ultracold atomic gases, providing experimental access to quantum gravity phenomenology at accessible energy scales.

1.10 Summary and Forward Look

1.10.1 Chapter Summary

This chapter formalized nodespace theory:

- **Graph-Theoretic Foundations**: Nodespace as directed graph (V, E, w)
- **Connectivity Matrix**: Exponential decay $C_{ij} = \exp(-d_{\text{graph}}/\lambda_{\text{node}})$
- **Emergence of Spacetime**: Metric $g_{\mu\nu}$ from connectivity via Regge calculus
- **Nodespace Dynamics**: Hamiltonian evolution, quantum fluctuations
- **Experimental Signatures**: CMB low-l suppression, fractal LSS, GW dispersion

1.10.2 Integration with Genesis Framework

Nodespace provides the substrate upon which:

- **Origami Dimensions** (Chapter **??**) fold and unfold
- **Meta-Principle Superforce** (Chapter **??**) governs evolution
- **Consciousness Resonance** emerges from network dynamics

1.10.3 Next Chapter

Chapter ??: Origami Dimensions develops dimensional folding mechanisms, fractal dimensions, and the 2D $\to$ 3D $\to$ 4D $\to$ nD progression.